Nonlin. Processes Geophys. Discuss., 1, 1803–1832, 2014
www.nonlin-processes-geophys-discuss.net/1/1803/2014/
doi:10.5194/npgd-1-1803-2014

Nonlinear Processes in Geophysics
Discussions
Open Access

Benjamin–Feir instability of waves in the presence of current

I. V. Shugan, H. H. Hwung, and R. Y. Yang

International Wave Dynamics Research Center, National Cheng Kung University, Tainan, Taiwan

Received: 7 November 2014 – Accepted: 10 November 2014 – Published: 5 December 2014

Correspondence to: I. V. Shugan (ishugan@rambler.ru)

Published by Copernicus Publications on behalf of the European Geosciences Union & the American Geophysical Union.

Abstract

The development of Benjamin–Feir instability of Stokes waves in the presence of variable current is presented. We employ a model of a resonance system having three coexisting nonlinear waves and nonuniform current. The model is free from the narrow-band approximation for surface waves and relatively weak adverse current. The modulation instability of Stokes waves in nonuniform moving media has special properties. Interaction with countercurrent accelerates the growth of sideband modes on a short spatial scale. An increase in initial wave steepness intensifies the wave energy exchange accompanied by wave breaking dissipation, results in asymmetry of sideband modes and a frequency downshift with an energy transfer jump to the lower sideband mode, and depresses the higher sideband and carrier wave. Nonlinear waves may even overpass the blocking barrier produced by strong adverse current. The frequency downshift of the energy peak is permanent and the system does not revert to its initial state. We find reasonable correspondence between the results of model simulations and available experimental results for wave interaction with blocking opposing current. Large transient or freak waves with amplitude and steepness several times those of normal waves may form during temporal nonlinear focusing of the resonant waves accompanied by energy income from sufficiently strong opposing current. We employ the resonance model for the estimation of the maximum amplification of wave amplitudes as a function of gradually increasing opposing current and compare the result obtained with recently published experimental results and modeling results obtained with the nonlinear Schrödinger equation.

1 Introduction

The problem of the interaction of a nonlinear wave with large-scale current remains an enormous challenge in physical oceanography. In spite of numerous papers devoted to the analysis of the phenomenon, some of the relatively strong effects still await

NPGD
1, 1803–1832, 2014

a clear description. The phenomenon can be considered as the discrete evolution of the spectrum of the surface wave under the influence of nonuniform adverse current. Experiments conducted by Chavla and Kirby (2002) and Ma et al. (2010) revealed that sufficiently steep surface waves overpass the barrier of strong opposing current on the lower resonant Benjamin–Feir sideband. These reports highlight that the frequency step of a discrete downshift coincides with the frequency step of modulation instability; i.e., after some distance of wave run, the maximum of the wave spectrum shifts in frequency to the lower sideband. The intensive exchange of wave energy produces a peak spectrum transfer jump, which is accompanied by essential wave breaking dissipation. The spectral characteristics of the initially narrow-band nonlinear surface wave packet dramatically change and the spectral width is increased by dispersion induced by the strong nonuniform current.

This paper considers a model of wave resonance in the presence of large-scale variable current with strong emphasis on the development of Benjamin–Feir (BF) instability without restrictions placed on the strength of current and the spectral width of the wave modulation.

Modulational instability (BF instability) (Benjamin and Feir, 1967) is a fundamental principle of nonlinear water wave dynamics. This phenomenon is of the utmost importance for the description of dynamics and downshifting of the energy spectrum among sea surface waves, the formation of freak (or giant) waves in oceans and wave breaking. In modern nonlinear physics, BF instability is considered as a basic process that classifies the qualitative behavior of modulated waves ("envelope waves") and may initialize the formation of stable entities such as envelope solitons.

The stationary nonlinear Stokes wave is unstable in response to perturbation of two small neighboring sidebands. The initial exponential growth of the two dominant sidebands at the expense of the primary wave gives rise to an intriguing Fermi–Pasta–Ulam recurring phenomenon of the initial state of wave trains. This phenomenon is characterized by a series of modulation–demodulation cycles in which initially uniform wave trains become modulated and then demodulated until they are again uniform (Lake

NPGD
1, 1803–1832, 2014

et al., 1978). However, when the initial slope is sufficiently steep, the long-time evolution of the wave train is different. The evolving wave trains experience strong modulations followed by demodulation, but the dominant component is the component at the frequency of the lower sideband of the original carrier. This is the temporary frequency downshift phenomenon. In systematic well-controlled experiments, Tulin and Waseda (1999) analyzed the effect of wave breaking on downshifting, high-frequency discretized energy, and the generation of continuous spectra. Experimental data clearly show that the active breaking process increases the permanent frequency downshift in the latter stages of wave propagation.

The BF instability of Stokes waves and its physical applications have been studied in depth over the last few decades; a long but incomplete list of research is Lo and Mei (1985), Osborne et al. (2000), Trulsen et al. (2000), Janssen (2003), Segur et al. (2005), Zakharov et al. (2006), Bridges and Dias (2007), Hwung et al. (2007), Shemer (2010), and Hwung et al. (2011). The latter stages of one cycle of the modulation process have been much less investigated, and many physical phenomena that have been observed experimentally still require extended theoretical analysis.

Modulation instability and the nonlinear interactions of waves are strongly affected by variable horizontal currents. Here, we face another fundamental problem of the mechanics of water waves – interactions with long-scale current. The effect of opposing current on waves is a problem of practical importance at tidal inlets and river mouths.

Even linear refraction of waves on currents can affect the wave field structure in terms of the direction and magnitude of waves. Waves propagating against an opposing current may have reduced wavelength and increased wave height and steepness.

If the opposing current is sufficiently strong, then the absolute group wave velocity in the stationary frame will become zero, resulting in the waves being blocked. This is the most intriguing phenomenon in the problem of wave–current interaction (Phillips, 1977). The kinematics condition for wave blocking can be written as

$$c_g + U(X) \to 0,$$

NPGD
1, 1803–1832, 2014

where c_g is the intrinsic group velocity of waves in a moving frame and $U(X)$ is slowly varying horizontal current, with X being the horizontal coordinate in the direction of wave propagation. Waves propagating against opposing current are stopped if the magnitude of the current, in the direction of wave propagation, exceeds the group velocity of the oncoming waves. This characteristic feature of wave blocking has drawn the interest of oceanographers and coastal engineers alike for its ability to be used as signature patterns of underlying large-scale motion (e.g., fresh water plumes and internal waves) and for the navigational hazard it poses. Smith (1975), Peregrine (1976), and Lavrenov (1998) analyzed refraction/reflection around a blocking region and obtained a uniformly valid linearized solution, including a short reflecting wave.

The linear modulation model has a few serious limitations. The most important is that the model predicts the blocking point according to the linear dispersion relation and cannot account for nonlinear dispersive effects. Amplitude dispersion effects can considerably alter the location of wave blocking predicted by linear theory, and nonlinear processes can adversely affect the dynamics of the wave field beyond the blocking point.

Donato et al. (1999), Stocker and Peregrine (1999), and Moreira and Peregrine (2012) conducted fully nonlinear computations to analyze the behavior of a train of water waves in deep water when meeting nonuniform currents, especially in the region where linear solutions become singular. The authors employed spatially periodic domains in numerical study and showed that adverse currents induce wave steepening and breaking. A strong increase in wave steepness is observed within the blocking region, leading to wave breaking, while wave amplitudes decrease beyond this region. The nonlinear wave properties reveal that at least some of the wave energy that builds up within the blocking region can be released in the form of partial reflection (which applies to very gentle waves) and wave breaking (even for small-amplitude waves).

The enhanced nonlinear nature of sideband instabilities in the presence of strong opposing current has also been confirmed by experimental observations. Chavla and Kirbi (2002) experimentally showed that the blockage phenomenon strongly depends

NPGD
1, 1803–1832, 2014

on the initial wave steepness; i.e., waves are blocked when the initial slope is gradual ($ak < 0.16$, where a and k are the wave amplitude and wave number, respectively). When the slope is sufficiently steep ($ak > 0.22$), the behavior of waves is principally different; i.e., waves are blocked only partly and frequency-downshifted waves overpass the blocking barrier. The lower sideband mode may dramatically increase; i.e., the amplitude may increase several times within a distance of a few wavelengths.

Wave propagation against nonuniform opposing currents was recently investigated in experiments conducted by Ma et al. (2010). Results confirm that opposing current not only increases the wave steepness but also shortens the wave energy transfer time and accelerates the development of sideband instability. A frequency downshift, even for very gradual initial steepness, was identified. Because of the frequency downshift, waves are more stable and have the potential to grow higher and propagate more quickly. The ultimate frequency downshift increases with an increase in initial steepness.

The wave modulation instability with coexisting variable current is commonly described theoretically by employing different forms of the modified nonlinear Schrödinger (NLS) equation. Gerber (1987) used the variational principle to derive a cubic Schrödinger equation for a nonuniform medium, limiting to potential theory in one horizontal dimension. Stocker and Peregrine (1999) extended the modified nonlinear NLS equation of Dysthe (1979) to include a prescribed potential current. Hjelmervik and Trulsen (2009) derived an NLS equation that includes waves and currents in two horizontal dimensions allowing weak horizontal shear. The horizontal current velocities are assumed just small enough to avoid collinear blocking and reflection of the waves.

Even though the frequency downshift and other nonlinear phenomena were observed in previous experimental studies on wave–current interactions, the theoretical description of the modulation instability of waves on opposing currents is not yet complete. An interaction of an initially relatively steep wave train with strong current nevertheless may abruptly transfer energy between the resonantly interacting harmon-

NPGD
1, 1803–1832, 2014

ics. Such wave phenomena are beyond the applicability of NLS-type models and await a theoretical description.

Another topic of practical interest in wave–current interaction problems is the appearance of large transient or freak waves with great amplitude and steepness owing to the focusing mechanism (e.g. Peregrine, 1976; Lavrenov, 1998; White and Fornberg, 1998; Kharif and Pelinovsky, 2006; Janssen, 2009; Ruban, 2012). Both nonlinear instability and refractive focusing have been identified as mechanisms for extreme-wave generation and these processes are generally concomitant in oceans and potentially act together to create giant waves.

Toffoli et al. (2013) showed experimentally that an initially stable surface wave can become modulationally unstable and even produce freak or giant waves when meeting negative horizontal current. Onorato et al. (2011) suggested an equation for predicting the maximum amplitude A_{max} during the wave evolution of currents in deep water. Their numerical results revealed that the maximum amplitude of the freak wave depends on U/c_g, where U is the velocity of the current and c_g is the group velocity of the wave packet.

Recently, Ma et al. (2013) experimentally investigated the maximum amplification of the amplitude of a wave on opposing current having variable strength at an intermediate water depth. They mentioned that theoretical values of amplification (Onorato et al., 2011; Toffoli et al., 2013) are essentially overestimated, probably owing to the effects of finite depth and wave breaking.

To address the abovementioned problems, we present a third-order resonance model of BF instability in the presence of horizontal long-scale current of variable strength. We analyze the interactions of a nonlinear surface wave with sufficiently strong opposing blocking current and the frequency downshifting phenomenon. The maximum amplification of the amplitude of surface waves is estimated for gradually increasing opposing current. We take into account the dissipation effects due to wave breaking and explore the threshold modification of the Tulin wave breaking model (Tulin,

NPGD
1, 1803–1832, 2014

1996; Huang et al., 2011). The results of model simulations are compared with available experimental results and theoretical estimations.

The paper consists of five sections. General modulation equations that describe the one-dimensional interaction of a triad of resonant surface waves and nonuniform current are derived in Sect. 2. Section 3 analyzes stationary nondissipative solutions for adverse and following nonuniform currents and various initial steepness of the surface wave train. We calculate the maximum amplitude amplification along gradually increasing opposing current and compared it with available experimental and theoretical results (Toffoli et al., 2013; Ma et al., 2013). The interaction of steep surface waves with strong adverse current under wave-blocking conditions including wave breaking effects is presented in Sect. 4. Modeling results are compared with the results of a series of experiments conducted by Chavla and Kirby (2002) and Ma et al. (2010). Section 5 summarizes our final conclusions and discussion.

2 Modulation equations for one-dimensional interaction

The first set of complete equations that describe short waves propagating over nonuniform currents of much larger scale were given by Longuet-Higgins and Stewart (1964). Wave energy is not conserved, and the concept of "radiation stress" was introduced to describe the average momentum flux in terms that govern the interchange of momentum with the current. In this model, it is also justifiable to neglect the effect of momentum transfer on the form of the surface current because it is an effect of the highest order (Stocker and Peregrine, 1999).

We construct a model of the current effect on the modulation instability of a nonlinear Stokes wave by making the following assumptions.

i. Surface waves and current propagate along a common x direction.

NPGD
1, 1803–1832, 2014

ii. By a_c, k_c and ω_c we denote the characteristic amplitude, wave number and angular frequency of the surface waves. We use a small conventional average wave steepness parameter; $\varepsilon = a_c k_c \ll 1$.

iii. The characteristic spatial scale used in developing the BF instability of the Stokes wave is l_c/ε^2, where $l_c = 2\pi/k_c$ is the typical wavelength of surface waves (Benjamin and Feir, 1967). We consider long-scale slowly varying current $U(x)$ with horizontal length scale L of the same order: $L = O(l_c/\varepsilon^2)$.

iv. It is assumed that the $U(x)$ dependence is due to the inhomogeneity of the bottom profile $h(x)$, which is sufficiently deep so that the deep-water regime for surface waves is ensured; i.e., $\exp(-2k_c h) \ll 1$. The characteristic current length L at which the function $U(x)$ varies noticeably is assumed to be much larger than the depth of the fluid, $h(x) \ll L$. Under these conditions, $U(x)h(x)$ is approximately constant, and the vertical component of the steady velocity field on the surface $z = \eta(x)$ can be neglected. This velocity field is directed along a tangent, and the slope of the tangent in the cases considered is negligibly small; i.e., $\eta'(x) \ll 1$. Correspondingly, it follows from the Bernoulli time-independent equation that the surface displacement induced by the current is small (Ruban, 2012). Such a situation can occur, for example, near river mouths or in tidal/ebb currents.

In all following equations, variables and sizes are scaled according to the above assumptions, and made dimensionless using the characteristic length and time scales of the wave field.

The zero-dimensional set of equations for potential motion of an ideal incompressible deep-depth fluid with a free surface in the presence of current $U(x)$ is given by the Laplace equation:

$$\varphi_{xx} + \varphi_{zz} = 0, \quad -h(x) < z < \varepsilon\eta(x,t). \tag{1}$$

NPGD
1, 1803–1832, 2014

The boundary conditions at the free surface are

$$-\eta = \varphi_t + U\varphi_x + \varepsilon\frac{1}{2}(\varphi_x^2 + \varphi_z^2), \quad z = \varepsilon\eta(x,t), \tag{2}$$

$$\eta_t + U\eta_x + \varepsilon\phi_x\eta_x = \phi_z, \quad z = \varepsilon\eta(x,t), \tag{3}$$

and those at the bottom are

$$\varphi \to 0, \quad z = -h(x). \tag{4}$$

Here, $\phi(x,z,t)$ is the velocity potential, $\eta(x,t)$ is the free-surface displacement, z is the vertical coordinate directed upward and t is time.

The variables are normalized as

$$\varphi = a_c\sqrt{\frac{g}{k_c}}\varphi' = \varepsilon\sqrt{\frac{g}{k_c^3}}\varphi', \quad \eta = a_c\eta' = \frac{\varepsilon}{k_c}\eta',$$
$$t = \frac{1}{\sqrt{gk_c}}t', \quad z = \frac{z'}{k_c}, \quad x = \frac{x'}{k_c}, \tag{5}$$
$$U(Kx) = U'(K/k_c x')c_\mathrm{p} = U'(\varepsilon^2 x')c_\mathrm{p},$$

where g is acceleration due to gravity, $K = 2\pi/L$, and c_p is the phase speed of the carrier wave, but the primes are omitted in Eqs. (1)–(4). Note that normalization Eq. (5) explicitly specifies the principal scales of sought functions φ and η.

The weakly nonlinear surface wave train is described by a solution to Eqs. (1)–(4), expanded into a Stokes series in terms of ε.

We will analyze the surface wave train as the almost-resonance wave triad of a particular form, which describes the development of modulation instability in the presence of current.

For calm water, the initially constant nonlinear Stokes wave with amplitude, wave number and frequency (a_1, k_1, σ_1) is unstable in response to a perturbation in the form

NPGD
1, 1803–1832, 2014

of a pair small waves with neighbor frequencies and wavenumbers: a superharmonic wave $(a_2, k_2 = k_1 + \Delta k, \sigma_2 = \sigma_1 + \Delta\sigma)$ and subharmonic wave $(a_0, k_0 = k_1 - \Delta k, \sigma_0 = \sigma_1 - \Delta\sigma)$. For most unstable modes, $\Delta\sigma/\sigma_1 = \varepsilon$ and $\Delta k/k_1 = 2\varepsilon$, where $\varepsilon = a_1 k_1$ is the initial steepness of the Stokes wave (Benjamin and Feir, 1967). This is the BF or modulation instability of the Stokes wave.

Kinematics resonance conditions for waves in the presence of slowly variable current are the same with one important particularity that intrinsic wave numbers and frequencies of resonance waves in the moving frame are variable and modulated by the current.

We analyze the problem assuming the wave motion phase $\theta_i = \theta_i(x,t)$ exists for each resonance wave in the presence of a slowly varying current $U(x)$, and we define the local wave number k_i and absolute observed frequency ω_i as

$$k_i = (\theta_i)_x, \quad \omega_i = \sigma_i + k_i U = -(\theta_i)_t, \quad i = 0,1,2. \tag{6}$$

For stationary modulation, the intrinsic frequency σ_i and wave number k_i for each wave slowly change in the presence of variable current, but the resonance condition

$$2\omega_1 \approx \omega_0 + \omega_2 \tag{7}$$

remains valid throughout the region of wave propagation owing to the stationary value of the absolute frequency for each of the harmonics.

The main kinematics wave parameters (σ_i, k_i) together with the first-order velocity potential amplitudes, φ_i, are considered further as slowly varying functions with typical scale, $O(\varepsilon^{-1})$, longer than the primary wavelength and period (Whitham, 1974):

$$\varphi_i = \varphi_i(\varepsilon x, \varepsilon t), k_i = k_i(\varepsilon x, \varepsilon t), \sigma_i = \sigma_i(\varepsilon x, \varepsilon t). \tag{8}$$

On this basis, we attempt to recover the effects of long-scale current and nonlinear wave dispersion (having the same order) additional to the Stokes term with the order of wave steepness squared.

NPGD
1, 1803–1832, 2014

The solution to the problem, uniformly valid for $O(\varepsilon^3)$, is found by a two-scale expansion with the differentiation:

$$\frac{\partial}{\partial t} = -\sum(\sigma_i + k_i U)\frac{\partial}{\partial \theta_i} + \varepsilon\frac{\partial}{\partial T},$$
$$\frac{\partial}{\partial x} = \sum k_i \frac{\partial}{\partial \theta_i} + \varepsilon\frac{\partial}{\partial X}, T = \varepsilon t, X = \varepsilon x. \quad (9)$$

Substitution of the wave velocity potential in its linear form,

$$\varphi = \sum_{i=0}^{i=2} \varphi_i e^{k_i z}\sin\theta_i, \quad (10)$$

satisfies the Laplace Eq. (1) to the first order of ε owing to Eq. (8) and gives the additional terms of the second order $O(\varepsilon^2)$:

$$\varepsilon(2k_i\varphi_{iX} + k_{iX}\varphi_i + 2k_i k_{iX}\varphi_i z)e^{k_i z}\cos\theta_i + \ldots = 0.$$

To satisfy the Laplace equation to second order, Yuen and Lake (1982), Shugan and Voliak (1998), and Hwung et al. (2010) suggested an additional phase-shifted term with a linear and quadratic z correction in the representation of the potential function φ:

$$\varphi = \sum_{i=0}^{i=2}\left(\varphi_i e^{k_i z}\sin\theta_i - \varepsilon\left(\varphi_{iX}z + \frac{k_{iX}\varphi_i}{2}z^2\right)e^{k_i z}\cos\theta_i\right) + \ldots. \quad (11)$$

Exponential decaying of the wave's amplitude with increasing $-z$ is accompanied by a second-order subsurface jet owing to slow horizontal variations in the wave number and amplitude of the wave packet.

The free-surface displacement $\eta = \eta(x,t)$ is also sought as an asymptotic series:

$$\eta = \eta_0 + \varepsilon\eta_1 + \varepsilon^2\eta_2 + \ldots, \quad (12)$$

NPGD
1, 1803–1832, 2014

where η_0, η_1, and η_2 are $O(1)$ functions to be determined. Using expressions (Eq. 10) and (Eq. 11) subject to the dynamic boundary condition (Eq. 2), we find the components of the free-surface displacement:

$$\eta_0 = \sum_{i=0}^{i=2} \sigma_i \varphi_i \cos\theta_i, \tag{13}$$

$$\eta_1 = -\sum_{i=0}^{i=2} (\varphi_{iT} \sin\theta_i + U\varphi_{iX} \sin\theta_i) + \sum_{i=0}^{i=2} \varphi_i^2 k_i^2 \cos[2\theta_i]/2$$
$$+ \sum_{i=0}^{i=2} \sum_{j\neq i}^{j=2} (\sigma_i - \sigma_j)^2 \sigma_i \sigma_j \varphi_i \varphi_j \cos[\theta_i - \theta_j]/2 \tag{14}$$
$$+ \sum_{i=0}^{i=2} \sum_{j\neq i}^{j=2} (\sigma_i + \sigma_j)^2 \sigma_i \sigma_j \varphi_i \varphi_j \cos[\theta_i + \theta_j]/2,$$

$$-8\eta_2 = \begin{pmatrix} \varphi_0\sigma_0^2(3\varphi_0^2\sigma_0^5 + 2\varphi_1^2\sigma_1^2(2\sigma_1^2 + \sigma_0^2)(2\sigma_1 - \sigma_0) \\ +2\varphi_2^2\sigma_2^2(2\sigma_2^2 + \sigma_0^2)(2\sigma_2 - \sigma_0))\cos[\theta_0] \\ +\varphi_1\sigma_1^2(3\varphi_1^2\sigma_1^5 + 2\varphi_0^2\sigma_0^2(2\sigma_0^2 + \sigma_1^2)(2\sigma_0 - \sigma_1) \\ +2\varphi_2^2\sigma_2^2(2\sigma_2^2 + \sigma_1^2)(2\sigma_2 - \sigma_1))\cos[\theta_1] \\ +\varphi_2\sigma_2^2(3\varphi_2^2\sigma_2^5 + 2\varphi_1^2\sigma_1^2(2\sigma_1^2 + \sigma_2^2)(2\sigma_1 - \sigma_2) \\ +2\varphi_0^2\sigma_0^2(2\sigma_0^2 + \sigma_2^2)(2\sigma_0 - \sigma_2))\cos[\theta_2] \\ -\varphi_0\varphi_1^2\sigma_0\sigma_1^2(\sigma_0^2 + 2\sigma_1^2)(\sigma_0^2 - 4\sigma_0\sigma_1 + 2\sigma_1^2)\cos[\theta_2 + \phi] \\ -\varphi_1^2\varphi_2\sigma_1^2\sigma_2(\sigma_2^2 + 2\sigma_1^2)(\sigma_2^2 - 4\sigma_2\sigma_1 + 2\sigma_1^2)\cos[\theta_0 + \phi] \\ -2\varphi_0\varphi_1\varphi_2\sigma_0\sigma_1\sigma_2(\sigma_0^2 + \sigma_1^2 + \sigma_2^2)(\sigma_0^2 - 2\sigma_0\sigma_1 + \sigma_1^2 - 2\sigma_1\sigma_2 + \sigma_2^2) \\ \cos[\theta_1 - \phi] \end{pmatrix}, \tag{15}$$

NPGD
1, 1803–1832, 2014

where ϕ is a slowly varying phase-shift difference: $\phi = 2\theta_1 - \theta_0 - \theta_2$.

Only the resonance terms for all three wave modes are included in the third-order displacement (15).

Substitution of the velocity potential (11) and displacement (13)–(15) into the kinematics boundary condition (3) gives, after much routine algebra, relationships between the modulation characteristics of the resonant wave:

$$\begin{cases} \sigma_0^2 = k_0 + \varepsilon^2\sigma_0^3(\varphi_0^2\sigma_0^5 + \varphi_1^2\sigma_1^3(2\sigma_1^2 - \sigma_0\sigma_1 + \sigma_0^2) + \varphi_2^2\sigma_2^3(2\sigma_2^2 - \sigma_0\sigma_2 + \sigma_0^2)) \\ \quad + \dfrac{\varepsilon^2\varphi_1^2\varphi_2\sigma_1^3\sigma_2^2}{\varphi_0}(2\sigma_1^3 - 2\sigma_1^2\sigma_2 + 2\sigma_1\sigma_2^2 - \sigma_2^3)\cos[\phi]; \\ \sigma_2^2 = k_2 + \varepsilon^2\sigma_2^3(\varphi_2^2\sigma_2^5 + \varphi_0^2\sigma_0^3(2\sigma_0^2 - \sigma_0\sigma_2 + \sigma_2^2) + \varphi_1^2\sigma_1^3(2\sigma_1^2 - \sigma_1\sigma_2 + \sigma_2^2)) \\ \quad + \dfrac{\varepsilon^2\varphi_1^2\varphi_0\sigma_1^3\sigma_0^2}{\varphi_2}(2\sigma_1^3 - 2\sigma_0\sigma_1^2 + 2\sigma_0^2\sigma_1 - \sigma_0^3)\cos[\phi]; \\ \sigma_1^2 = k_1 + \varepsilon^2\sigma_1^3(\varphi_1^2\sigma_1^5 + \varphi_0^2\sigma_0^3(2\sigma_0^2 - \sigma_0\sigma_1 + \sigma_1^2) + \varphi_2^2\sigma_2^3(\sigma_1^2 - \sigma_1\sigma_2 + 2\sigma_2^2)) \\ \quad + \varepsilon^2\varphi_0\varphi_2\sigma_0\sigma_1^2\sigma_2(\sigma_0^4 - \sigma_0^3\sigma_1 - \sigma_0\sigma_1(\sigma_1 - \sigma_2)^2 \\ \quad + \sigma_0^2(\sigma_1^2 - \sigma_1\sigma_2 + 2\sigma_2^2) + \sigma_2(-\sigma_1^3 + \sigma_1^2\sigma_2 - \sigma_1\sigma_2^2 + \sigma_2^3))\cos[\phi]; \end{cases} \tag{16}$$

$$\begin{cases} [\phi_0^2\sigma_0^2]_T + \left[(U(X) + \dfrac{1}{2\sigma_0})\phi_0^2\sigma_0^2\right]_X \\ = \varepsilon\phi_1^2\phi_2\phi_0\sigma_1^3\sigma_2^2(2\sigma_1^3 - 2\sigma_1^2\sigma_2 + 2\sigma_1\sigma_2^2 - \sigma_2^3)\sin[\varphi] - \phi_0^2\sigma_0U'(X)/2; \\ [\phi_2^2\sigma_2^2]_T + \left[(U(X) + \dfrac{1}{2\sigma_2})\phi_2^2\sigma_2^2\right]_X \\ = \varepsilon\phi_1^2\phi_2\phi_0\sigma_0^2\sigma_1^3(2\sigma_1^3 - 2\sigma_0\sigma_1^2 + 2\sigma_0^2\sigma_1 - \sigma_0^3)\sin[\varphi] - \phi_2^2\sigma_2U'(X)/2; \\ [\phi_1^2\sigma_1^2]_T + \left[(U(X) + \dfrac{1}{2\sigma_1})\phi_1^2\sigma_1^2\right]_X \\ = -\varepsilon\phi_1^2\phi_2\phi_0\sigma_0\sigma_1^2\sigma_2(\sigma_0^4 - \sigma_0^3\sigma_1 - \sigma_0\sigma_1(\sigma_1 - \sigma_2)^2 + \\ \sigma_0^2(\sigma_1^2 - \sigma_1\sigma_2 + 2\sigma_2^2) - \sigma_2(\sigma_1^3 - \sigma_1^2\sigma_2 + \sigma_1\sigma_2^2 - \sigma_2^3))\sin[\varphi] - \phi_1^2\sigma_1U'(X)/2. \end{cases} \tag{17}$$

NPGD
1, 1803–1832, 2014

The Eq. (16) represent the "intrinsic" dispersion relations of the nonlinear wave for each of the resonant harmonics in the presence of current, $U(X)$. Equation (17) yields the known wave energy law with the energy exchange terms and sink/source term of the wave obtained from the current variability on the right side of the equations. Modulation Eqs. (16) and (17) are closed by the equations of wave phase conservation that follow from Eq. (5) as the compatibility condition (Phillips, 1977):

$$k_{iT} + (\sigma_i + k_i U)_X = 0, \quad i = 0,1,2. \tag{18}$$

The derived set of nine modulation Eqs. (16)–(18) form the complete system for nine unknown functions $(k_i, \sigma_i, \varphi_i, i = 0,1,2)$.

3 Nondissipative stationary-wave modulations

Let us analyze the stationary-wave solutions of the problem (Eqs. 16–18) supposing that all unknown functions depend on the single coordinate X. Then, after integrating Eq. (18), we have the conservation law for the absolute frequency of each wave:

$$\sigma_i + k_i U = \omega_i = \text{const}, \quad i = 0,1,2. \tag{19}$$

NPGD
1, 1803–1832, 2014

The wave energy laws for resonant components take the form

$$\begin{cases} \left[(U+\frac{1}{2\sigma_0})\phi_0^2\sigma_0^2\right]_X = \varepsilon\phi_1^2\phi_2\phi_0\sigma_1^3\sigma_2^2(2\sigma_1^3-2\sigma_1^2\sigma_2+2\sigma_1\sigma_2^2-\sigma_2^3)\sin[\varphi] \\ -\phi_0^2\sigma_0U'(X)/2 \\ \left[(U+\frac{1}{2\sigma_2})\phi_2^2\sigma_2^2\right]_X = \varepsilon\phi_1^2\phi_2\phi_0\sigma_1^3\sigma_0^2(2\sigma_1^3-2\sigma_0\sigma_1^2+2\sigma_0^2\sigma_1-\sigma_0^3)\sin[\varphi] \\ -\phi_2^2\sigma_2U'(X)/2 \\ \left[(U+\frac{1}{2\sigma_1})\phi_1^2\sigma_1^2\right]_X = -\varepsilon\phi_1^2\phi_2\phi_0\sigma_0\sigma_1^2\sigma_2(\sigma_0^4-\sigma_0^3\sigma_1-\sigma_0\sigma_1(\sigma_1-\sigma_2)^2+ \\ \sigma_0^2(\sigma_1^2-\sigma_1\sigma_2+2\sigma_2^2)-\sigma_2(\sigma_1^3-\sigma_1^2\sigma_2+\sigma_1\sigma_2^2-\sigma_2^3))\sin[\varphi]-\phi_1^2\sigma_1U'(X)/2 \end{cases} . \quad (20)$$

Typical behavior of wave instability in the absence of current is presented in Fig. 1a for a Stokes wave having initial steepness $\varepsilon = 0.1$. Two initially negligible side bands (II) and (III) exponentially grow at the expense of the main Stokes wave (I), and after saturation, the wave system reverts to its initial state, which is the Fermi–Pasta–Ulam recurrence phenomenon. One can see here also the characteristic spatial scale for the developing of modulation instability $O(1/(k_c\varepsilon^2))$.

The development of modulation instability on negative variable current $U = U_0\mathrm{Sech}\left[\varepsilon^2(x-200)\right], U_0 = -0.1$, is presented in Fig. 1b. The modulation instability develops far more quickly on opposing current and reaches deeper stages of modulation. The energetic process is described as follows. The basic Stokes wave (I) absorbs energy from the counter current U and its steepness increases. This in turn accelerates the wave instability; there is a corresponding increase in energy flow to the most unstable sideband modes (II) and (III). The linear modulation model (Gargett and Hughes, 1972; Lewis et al., 1974) has a much larger maximum amplitude of the carrier wave (IV).

The region of the most developed instability corresponds to the spatial location of the maximum of the negative current (Fig. 1c). The counter energy flows from the current

NPGD
1, 1803–1832, 2014

and the other resonant waves give rise to mutual oscillations for all wave amplitudes (I)–(III).

The opposite scenario of copropagating current is presented in Fig. 1d. The modulation instability is depressed by the following current $U(X) > 0$ and the resonant sideband modes develop at a distance from the origin that is almost twice that in the case of no current.

The increasing strength of the opposing flow ($U_0 = -0.2$) results in deeper modulation of waves and more frequent mutual oscillations of the amplitudes (Fig. 1e). There are essential oscillations of wave-number functions of the sideband modes (II) and (III) (Fig. 1f) owing to the nonlinear dispersion properties of waves. We mention also that the wave number of the carrier wave in the linear model (IV) is much higher than that in the nonlinear model (I). The width of the wave-number spectrum of the wave train in the nonlinear model locally increases to almost twice the initial width.

To estimate the possibility of generating large transient waves, we employ the resonance model and calculate the maximum amplification of the amplitudes of surface waves on linearly increasing opposing current. The boundary conditions for the unperturbed waves were taken from experiments conducted by Toffoli et al. (2013) and Ma et al. (2013). Results of calculations are presented in Fig. 2a and b.

Qualitatively, the results of both tests conducted by Toffoli et al. (2013) (Fig. 2a) are in good agreement with the theory presented by Onorato et al. (2011). The resonant model slightly overestimates the experimental values. However, observations made by Ma et al. (2013) (Fig. 2b) are notably overestimated by the theory of Onorato et al. (2011) and resonance-model simulations are in far greater agreement with the experimental values.

4 Wave propagation under the blocking conditions of strong adverse current

Stokes waves with sufficiently high initial steepness ε under the impact of strong blocking adverse current ($U(X) < -C_g$) will inevitably reach the breaking threshold for the

NPGD
1, 1803–1832, 2014

steepness of water waves. We include breaking dissipation effects in this case. We employ the adjusted dissipative model of Tulin (1996) and Huang et al. (2011) to describe the effect of breaking on the dynamics of the water wave. An analysis of fetch laws parameterized by Tulin reveals that the rate of energy loss due to breaking is of fourth order of the wave amplitude:

$$D_a/e = \omega D \eta^2 k^2,$$

where e is the wave energy density and $D = O(10^{-1})$ is a small empirical constant.

The sink of energy and momentum due to wave breaking leads to additional terms on the right sides of the wave energy Eq. (20) and dispersive Eq. (16) for each wave. Tulin (1996) suggested using sink terms along the entire path of wave interaction with the wind. The wave dissipation function for the adjusted model (Huang et al., 2011) includes also the wave steepness threshold function

$$H\left[\frac{|A_X|}{A_S} - 1\right],$$

where H is the Heaviside unit step function, and A_S is the threshold value of the characteristic steepness $A_X = \varepsilon \sum \sigma_i \varphi_i k_i$, which is the function applied to calculate energy and momentum losses.

NPGD
1, 1803–1832, 2014

The dispersion relation (Eq. 16) and wave energy laws (Eq. 20) including break dissipation take the form

$$
\begin{cases}
\sigma_0^2 = k_0 + \varepsilon^2\sigma_0^3(\phi_0^2\sigma_0^5 + \phi_1^2\sigma_1^3(2\sigma_1^2 - \sigma_0\sigma_1 + \sigma_0^2) + \phi_2^2\sigma_2^3(2\sigma_2^2 - \sigma_0\sigma_2 + \sigma_0^2)) \\
\qquad + \dfrac{\varepsilon^2\phi_1^2\phi_2\sigma_1^3\sigma_2^2}{\phi_0}(2\sigma_1^3 - 2\sigma_1^2\sigma_2 + 2\sigma_1\sigma_2^2 - \sigma_2^3)\cos[\varphi] \\
\qquad + \varepsilon^2 H[\chi]\left\{ \begin{array}{l} D\sin[\varphi]\phi_1^2\phi_2/\phi_0 k_0^4 + 8\gamma D\varepsilon^2 X(\phi_0^2 + \phi_1^2 + \phi_2^2) \\ -4\gamma D\phi_1^2\phi_2/\phi_0 \sin[\varphi]\varepsilon/(k_2 - k_1) \end{array} \right\}; \\
\sigma_2^2 = k_2 + \varepsilon^2\sigma_2^3(\phi_2^2\sigma_2^5 + \phi_0^2\sigma_0^3(2\sigma_0^2 - \sigma_0\sigma_2 + \sigma_2^2) + \phi_1^2\sigma_1^3(2\sigma_1^2 - \sigma_1\sigma_2 + \sigma_2^2)) \\
\qquad + \dfrac{\varepsilon^2\phi_1^2\phi_0\sigma_1^3\sigma_0^2}{\phi_2}(2\sigma_1^3 - 2\sigma_0\sigma_1^2 + 2\sigma_0^2\sigma_1 - \sigma_0^3)\cos[\varphi] \\
\qquad + \varepsilon^2 H[\chi]\left\{ \begin{array}{l} D\sin[\varphi]\phi_1^2\phi_0/\phi_2 k_2^4 + 8\gamma D\varepsilon^2 X(\phi_0^2 + \phi_1^2 + \phi_2^2) \\ +4\gamma D\phi_1^2\phi_0/\phi_2 \sin[\varphi]\varepsilon/(k_1 - k_0) \end{array} \right\}; \\
\sigma_1^2 = k_1 + \varepsilon^2\sigma_1^3(\phi_1^2\sigma_1^5 + \phi_0^2\sigma_0^3(2\sigma_0^2 - \sigma_0\sigma_1 + \sigma_1^2) + \phi_2^2\sigma_2^3(\sigma_1^2 - \sigma_1\sigma_2 + 2\sigma_2^2)) \\
\qquad + \varepsilon^2\phi_0\phi_2\sigma_0\sigma_1^2\sigma_2(\sigma_0^4 - \sigma_0^3\sigma_1 - \sigma_0\sigma_1(\sigma_1 - \sigma_2)^2 + \sigma_0^2(\sigma_1^2 - \sigma_1\sigma_2 + 2\sigma_2^2) \\
\qquad + \sigma_2(-\sigma_1^3 + \sigma_1^2\sigma_2 - \sigma_1\sigma_2^2 + \sigma_2^3))\cos[\varphi] \\
\qquad + \varepsilon^2 H[\chi]\left\{ \begin{array}{l} -2D\sin[\varphi]\phi_2\phi_0 k_1^4 + 8\gamma D\varepsilon^2 X(\phi_0^2 + \phi_1^2 + \phi_2^2) \\ +4\gamma D\phi_2\phi_0 \sin[\varphi]\dfrac{(k_2 - 2k_1 + k_0)2\varepsilon}{(k_1 - k_0)(k_2 - k_1)} \end{array} \right\};
\end{cases}
\tag{21}
$$

NPGD
1, 1803–1832, 2014

where $\chi = |A_X|/A_S - 1$, and

$$\begin{cases} \left[(U(X) + \frac{1}{2\sigma_0})\phi_0^2\sigma_0^2\right]_X = \varepsilon\phi_1^2\phi_2\phi_0\sigma_1^3\sigma_2^2(2\sigma_1^3 - 2\sigma_1^2\sigma_2 + 2\sigma_1\sigma_2^2 - \sigma_2^3)\sin[\varphi] \\ -\phi_0^2\sigma_0 U'(X)/2 + \varepsilon H[\chi]\left\{\begin{array}{l} -k_0^4\phi_1^2\phi_2\phi_0 D\cos[\varphi] - k_0^4\phi_0^2(\phi_0^2 + 2\phi_1^2 + 2\phi_2^2) + \\ 4\gamma D\phi_0^2 k_0^4(\phi_1^2\varepsilon/(k_1 - k_0) + \phi_2^2 2\varepsilon/(k_2 - k_0) + \\ \phi_1^2\phi_2/\phi_0\cos[\varphi]\varepsilon/(k_2 - k_1)) \end{array}\right\}; \\ \left[(U(X) + \frac{1}{2\sigma_2})\phi_2^2\sigma_2^2\right]_X = \varepsilon\phi_1^2\phi_2\phi_0\sigma_1^3\sigma_0^2(2\sigma_1^3 - 2\sigma_0\sigma_1^2 + 2\sigma_0^2\sigma_1 - \sigma_0^3)\sin[\varphi] \\ -\phi_2^2\sigma_2 U'(X)/2 + \varepsilon H[\chi]\left\{\begin{array}{l} -k_2^4\phi_1^2\phi_2\phi_0 D\cos[\varphi] - k_2^4\phi_2^2(\phi_2^2 + 2\phi_0^2 + 2\phi_1^2) + \\ 4\gamma D\phi_2^2 k_2^4(\phi_1^2\varepsilon/(k_2 - k_1) + \phi_0^2 2\varepsilon/(k_2 - k_0) + \\ \phi_1^2\phi_0/\phi_2\cos[\varphi]\varepsilon/(k_1 - k_0)) \end{array}\right\}; \\ \left[(U(X) + \frac{1}{2\sigma_1})\phi_1^2\sigma_1^2\right]_X = -\varepsilon\phi_1^2\phi_2\phi_0\sigma_0\sigma_1^2\sigma_2(\sigma_0^4 - \sigma_0^3\sigma_1 - \sigma_0\sigma_1(\sigma_1 - \sigma_2)^2 \\ + \sigma_0^2(\sigma_1^2 - \sigma_1\sigma_2 + 2\sigma_2^2) - \sigma_2(\sigma_1^3 - \sigma_1^2\sigma_2 + \sigma_1\sigma_2^2 - \sigma_2^3))\sin[\varphi] \\ -\phi_1^2\sigma_1 U'(X)/2 + \varepsilon H[\chi]\left\{\begin{array}{l} -2k_1^4\phi_1^2\phi_2\phi_0 D\cos[\varphi] - k_1^4\phi_1^2(\phi_1^2 + 2\phi_0^2 + 2\phi_2^2) + \\ 4\gamma D\phi_1^2 k_1^4((\phi_2^2 - \phi_0^2)\varepsilon/(k_1 - k_0) + \\ \phi_2\phi_0\cos[\varphi](k_2 + k_0 - 2k_1)/(k_2 - k_1)\varepsilon/(k_2 - k_1)) \end{array}\right\}; \end{cases} \quad (22)$$

where empirical constant $\gamma = O(10^{-1})$.

We performed numerical simulations using the model for the boundary conditions and the form of the variable current obtained in two series of experiments conducted by Chavla and Kirby (2002) and Ma et al. (2010).

Data for the wave blocking regime in experiments conducted by Chavla and Kirby (2002) are taken from their Test 6 (Fig. 11). The experimental results of Test 6 and our

NPGD
1, 1803–1832, 2014

numerical simulation results are compared in Fig. 3. A surface wave with initially high steepness ($A_1 k_1 = 0.296$) and period $T = 1.2$ s meets adverse current with increasing amplitude.

The wave modeling has distinctive features that agree reasonably well with the results of experiments:

- initial symmetrical growth of the main sidebands with frequencies $f_0 = 0.688, f_2 = 0.978$ Hz at distances up to $k_1 x < -2$;
- asymmetrical growth of sidebands beginning at ($k_1 x \approx -2$) and downshifting of energy to the lower sideband;
- energy transfer at very short spatial distances and several times increases in the lower sideband amplitude just on a half meter length $k_1 x \in (-2, 0)$.
- a depressed higher frequency band and primary wave;
- an almost permanent increase in the lowest subharmonic along the tank;
- sharp accumulation of energy by the lowest subharmonic wave during interaction with increasing opposing current; and
- final permanent downshifting of the wave energy.

The presented third-order wave amplitude model agrees reasonably well with experimental results.

Modulation evolution of breaking waves in experiments of Ma et al. (2010) for the most intriguing case 3 are presented in Fig. 4 together with the results of our numerical computations. A primary wave with period $T = 1$ s and steepness $A_1 k_1 = 0.18$ meets linearly increasing opposing current that finally exceeds the threshold to be a linear blocking barrier for the primary wave $U(x) < -1/4C$. In experiments, sideband frequencies arose ubiquitously from the background noise of the flume. In numerical simulations, the sidebands were slightly seeded at frequencies corresponding to the most unstable

NPGD
1, 1803–1832, 2014

modes. The wave-breaking region in this experimental case ranged from $k_1 x = 52$ to $k_1 x = 72$. The lower sideband amplitude grew with increasing distance at the expense of the primary wave, while there was little change in the higher sideband energy. There was an effective frequency downshift following initial breaking ($k_1 x = 56$). The modeling results agree reasonably well with the experimental data.

5 Conclusions

A resonance system comprising three waves in nonuniform media gives rise to modulation instability with special properties. Interaction with countercurrent accelerates the growth of sideband modes on much shorter spatial scales. In contrast, wave instability on following current is sharply depressed. Amplitudes and wave numbers of all resonant waves vary enormously in the presence of strong adverse current. The steepness of a nonlinear wave on adverse current is much less than that of a linear refraction model.

Large transient or freak waves with amplitude and steepness several times larger than those of normal waves may form during temporal nonlinear focusing of the resonant waves accompanied by energy income from sufficiently strong opposing current. The amplitude of a rogue wave strongly depends on the ratio of the current velocity to group velocity.

Interaction of initially steep waves with the strong blocking adverse current results in intensive energy exchange between resonance components and energy downshifting to the lower sideband mode accompanied by active breaking. A more stable long wave with lower frequency can overpass the blocking barrier and accumulate almost all the wave energy of the packet. The frequency downshift of the energy peak is permanent and the system does not revert to its initial state.

A third-order dissipative wave resonant model satisfactorily agrees with available experimental data on the explosive instability of waves on blocking adverse current and the generation of rough waves.

NPGD
1, 1803–1832, 2014

Acknowledgements. The authors would like to thank the Ministry of Science and Technology of Taiwan (NSC 103-2911-I-006 -302 and to National Cheng-Kung University) and the Ministry of Education, Taiwan, R.O.C. The Aim for the Top University Project to the National Cheng Kung for financial support.

References

Benjamin, T. B. and Feir, J. E.: Instability of periodic wavetrains in nonlinear dispersive systems, J. Fluid Mech., 27, 417–430, 1967.

Bridges, T. and Dias, F.: Enhancement of the Benjamin-Feir instability with dissipation, Phys. Fluids., 19, 104104, doi:10.1063/1.2780793, 2007.

Chavla, A. and Kirby, J.: Experimental study of breaking waves on a blocking current, Proc. 26th International Conference on Coastal Engineering, Copenhagen, 22–26 June, 759–772, 1998.

Chavla, A. and Kirby, J.: Monochromatic and random wave breaking at block points, J. Geophys. Res., 107, 4.1–4.19, 2002.

Chabchoub, A., Akhmediev, N., and Hoffmann, N.: Experimental study of spatiotemporally localized surface gravity water waves, Phys. Rev. E, 86, 016311, doi:10.1103/PhysRevE.86.016311, 2012.

Dias, F. and Kharif, C.: Nonlinear gravity and capillary-gravity waves, Annu. Rev. Fluid Mech., 31, 301–346, 1999.

Donato, A. N., Peregrine, D. H., and Stocker, J. R.: The focusing of surface. waves by internal Waves, J. Fluid Mech., 384, 27–58, 1999.

Dysthe, K. B.: Note on a modification to the nonlinear Schrodinger equation for application to deep water waves, P. R. Soc. A, 369, 105–114, 1979.

Gargett, A. E. and Hughes, B. A.: On the interaction of surface and internal waves, J. Fluid Mech., 52, 179–191, 1972.

Gerber, M.: The Benjamin–Feir instability of a deep water Stokes wavepacket in the presence of a non-uniform medium, J. Fluid Mech., 176, 311–332, 1987.

Hjelmervik, K. B. and Trulsen, K.: Freak wave statistics on collinear currents, J. Fluid Mech., 637, 267–284, 2009.

NPGD

1, 1803–1832, 2014

Hwung, H., Chiang, W., and Hsiao, S.: Observations on the evolution of wave modulation, P. Roy. Soc. Lond. A. Mat., 463, 85–112, 2007.
Hwung, H., Yang, R., and Shugan, I.: Exposure of internal waves on the sea surface, J. Fluid Mech., 626, 1–20, 2009.
Hwung, H., Chiang, W., Yang, R., and Shugan, I.: Threshold Model on the Evolution of Stokes Wave Side-Band Instability, Eur. J. Mech. B-Fluid., 30, 147–155, 2011.
Janssen, P.: Nonlinear four-wave interactions and freak waves, J. Phys. Oceanogr., 33, 863–884, 2003.
Janssen, T. and Herbers, T.: Nonlinear Wave Statistics in a Focal Zone, J. Phys. Oceanogr., 39, 1948–1964, 2009.
Kharif, C. and Pelinovsky, E.: Freak waves phenomenon: physical mechanisms and modelling, in: Waves in Geophysical Fluids: CISM Courses and Lectures 489, edited by: Grue, J. and Trulsen, K., 107–172, New York, Springer Wein, 2006.
Lake, B. M. and Yuen, H. C.: A new model for nonlinear wind waves. Part 1. Physical model and experimental evidence, J. Fluid Mech., 88, 33–62, 1978.
Landrini, M., Oshri, O., Waseda, T., and Tulin, M. P.: Long time evolution of gravity wave systems, in: Proc. 13th Intl Workshop on Water Waves and Floating Bodies, edited by: Hermans,. A. J., Alphen aan den Rijn, 75–78, 1998.
Lavrenov, I. V.: The wave energy concentration at the Agulhas current off South Africa, Nat. Hazards, 17, 117–127, 1998.
Lewis, J. E., Lake, B. M., and Ko, D. R.: On the interaction of internal waves and surface gravity waves, J. Fluid Mech., 63, 773–800, 1974.
Lo, E. and Mei, C. C.: A numerical study of water-wave modulation base on a higher-order nonlinear Schrodinger equation, J. Fluid Mech., 150, 395–416, 1985.
Longuet-Higgins, M. and Stewart, R.: Radiation stresses in water waves: a physical discussion, with applications, Deep-Sea Res., 11, 529–562, 1964.
Ma, Y., Dong, G., Perlin, M., Ma, X., Wang, G., and Xu, J.: Laboratory observations of wave evolution, modulation and blocking due to spatially varying opposing currents, J. Fluid Mech., 661, 108–129, 2010.
Ma, Y., Ma, X., Perlin, M., and Dong, G.: Extreme waves generated by modulational instability on adverse currents, Phys. Fluids, 25, 114109, doi:10.1063/1.4832715, 2013.
Melville, W.: Wave modulation and breakdown, J. Fluid Mech., 128, 489–506, 1983.

NPGD
1, 1803–1832, 2014

Onorato, M., Proment, D., and Toffoli, A.: Triggering rogue waves in opposing currents, Phys. Rev. Lett., 107, 184502, doi:10.1103/PhysRevLett.107.184502, 2011.
Osborne, A.: The random and deterministic dynamics of rogue waves in unidirectional, deep-water wave trains, Mar. Struct., 14, 275–293, 2001.
Osborne, A.: Nonlinear Ocean Waves and the Inverse Scattering Transform, Elsevier, New York, 2010.
Osborne, A. R., Onorato, M., and Serio, M.: The nonlinear dynamics of rogue waves and holes in deep-water gravity wave trains, Phys. Lett. A, 275, 386–393, 2000.
Peregrine, D. H.: Interaction of water waves and currents, Adv. Appl. Mech., 16, 9–117, 1976.
Phillips, O. M.: Theoretical and Experimental Studies of Gravity wave interactions, P. Roy. Soc. Lond. A. Mat., 299, 104–119, 1967.
Phillips, O. M.: The Dynamics of the Upper Ocean, Cambridge University Press, Cambridge – London – New York – Melbourne, 1977.
Ruban, V.: On the Nonlinear Schrödinger Equation for waves on a nonuniform current, JETP. Lett., 95, 486–491, 2012.
Segur, H., Henderson, D., Hammack, J., Li, C.-M., Phei, D., and Socha, K.: Stabilizing the Benjamin–Feir instability, J. Fluid Mech., 539, 229–271, 2005.
Shemer, L.: On Benjamin-Feir instability and evolution of a nonlinear wave with finite-amplitude sidebands, Nat. Hazards Earth Syst. Sci., 10, 2421–2427, doi:10.5194/nhess-10-2421-2010, 2010.
Shemer, L., Kit, E., and Jiao, H.: An experimental and numerical study of the spatial evolution of unidirectional nonlinear water-wave groups, Phys. Fluids, 14, 3380–3390, 2002.
Shugan, I. and Voliak, K.: On phase kinks, negative frequencies and other third order peculiarities of modulated surface waves, J. Fluid Mech., 368, 321–338, 1998.
Smith, R.: Reflection of short gravity waves on a non-uniform current, Math. Proc. Cambridge, 78, 517–525, 1975.
Stiassnie, M. and Shemer, L.: On the interaction of four water-waves, Wave Motion, 41, 307–328, 2005.
Stocker, J. R. and Peregrine, D. H.: Three-dimensional surface. waves propagating over long internal waves, Eur. J. Mech. B-Fluid., 18, 545–559, 1999.
Toffoli, A., Waseda, T. Houtani, H., Kinoshita, T., Collins, K., Proment, D., and Onorato, M.: Excitation of rogue waves in a variable medium: An experimental study on the interaction

NPGD
1, 1803–1832, 2014

of water waves and currents, Phys. Rev. E, 87, 051201, doi:10.1103/PhysRevE.87.051201, 2013.
Trulsen, K., Kliakhandler, I., Dysthe, K., and Velarde, M.: On weakly nonlinear modulation of waves on deep water, Phys. Fluids, 12, 2432–2437, 2000.
Tulin, M. P.: Breaking of ocean waves and downshifting, in: Waves and Nonlinear Processes in Hydrodynamics, edited by: J. Grue, B. Gjevik, and J. E. Weber, 177–190, Kluwer, Kluwer, Dordrecht, 1996.
Tulin, M. P. and Waseda, T.: Laboratory observations of wave group evolution, including breaking effects, J. Fluid Mech., 378, 197–232, 1999.
White, B. and Fornberg, B.: On the chance of freak waves at sea, J. Fluid Mech., 355, 113–138, 1998.
Whitham, G. B.: Linear and Nonlinear Waves, John Wiley and Sons, New York, 1974.
Yuen, H. C. and Lake, B. M.: Nonlinear dynamics of deep-water gravity waves, Adv. Appl. Mech., 22, 67–229, 1982.
Ying, L., Zhuang, Z., Heller, E., and Kaplan, L.: Linear and nonlinear rogue wave statistics in the presence of random currents, Nonlinearity, 24, 67–87, 2011.
Zakharov, V., Dyachenko, A., and Prokofiev, A.: Freak waves as nonlinear stage of Stokes wave modulation instability, Eur. J. Mech. B-Fluid., 25, 677–692, 2006.

NPGD
1, 1803–1832, 2014

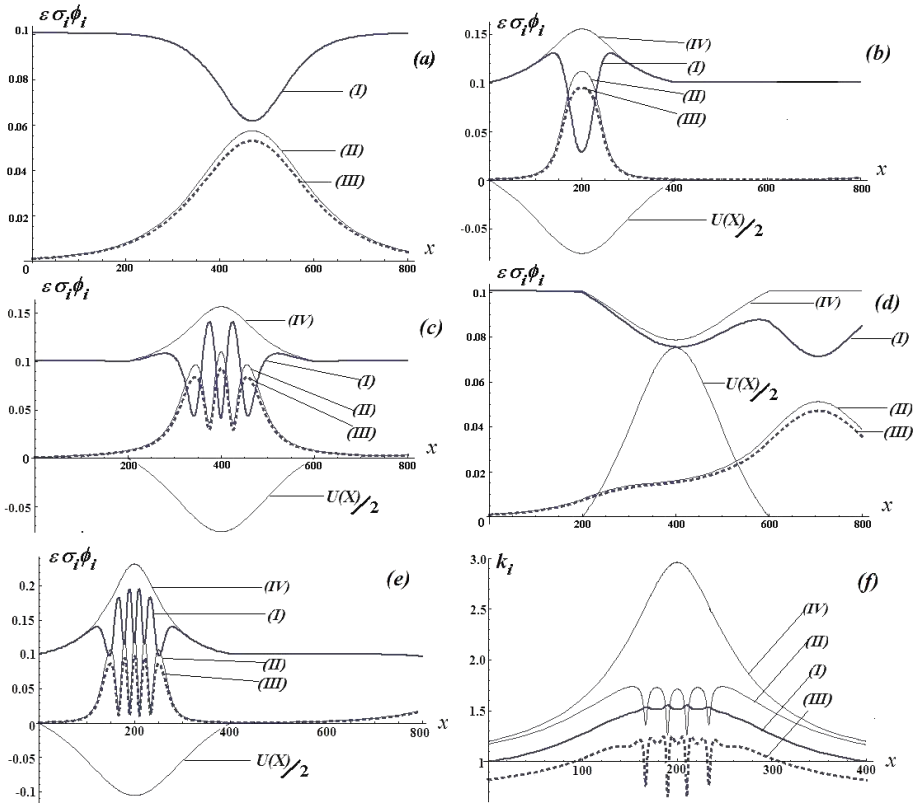

Figure 1. (a) BF instability without current. **(b)**, **(c)** Modulation of surface waves by adverse current $U = U_0 \mathrm{Sech}\left[\varepsilon^2(x - x_0)\right]$, ($U_0 = -0.1$), **(b)** $x_0 = 200$, **(c)** $x_0 = 400$. **(d)** Modulation instability for following current ($U_0 = 0.1, x_0 = 400$). **(e)**, **(f)** Functions of wave amplitude and wave number respectively for $U_0 = -0.2$. (I), (II), (III) Amplitude envelopes of the carrier, superharmonic and subharmonic waves, respectively. (IV) Linear solution for the carrier envelope. The initial steepness of the carrier wave is $\varepsilon = 0.1$.

NPGD
1, 1803–1832, 2014

Benjamin–Feir instability of waves in the presence of current

I. V. Shugan et al.

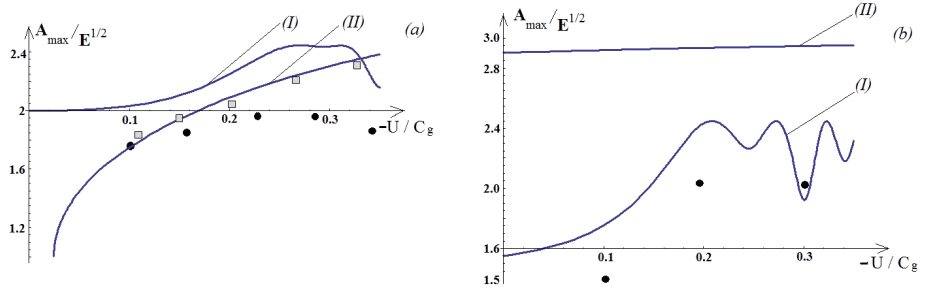

Figure 2. Nondimensional maximum wave amplitude as a function of U/C_g, where C_g is the group velocity of the carrier wave and $E^{1/2}$ is the local SD of the wave envelope.
(a) Experiments conducted by Toffoli et al. (2013) for carrier wave of period $T = 0.8$ s (wavelength $\lambda \cong 1$ m), initial steepness $k_1 a_1 = 0.063$, and frequency difference $\Delta\omega/\omega_1 = 1/11$. Solid dots show measurements made using a flume at Tokyo University and squares show results obtained at Plymouth University. Line (I) shows the resonance model prediction while line (II) shows the prediction made using Eq. (1) (Onorato et al., 2011).
(b) Case T11 in Ma et al. (2013) for carrier-wave frequency $\omega_1 = 1$ Hz, initial steepness $k_1 a_1 = 0.115$, and frequency difference $\Delta\omega/\omega_1 = 0.44 a_1 k_1$. Solid dots show measurements. Line (I) shows the resonance model prediction, while line (II) shows the prediction made using Eq. (15) (Onorato et al., 2011).

NPGD
1, 1803–1832, 2014

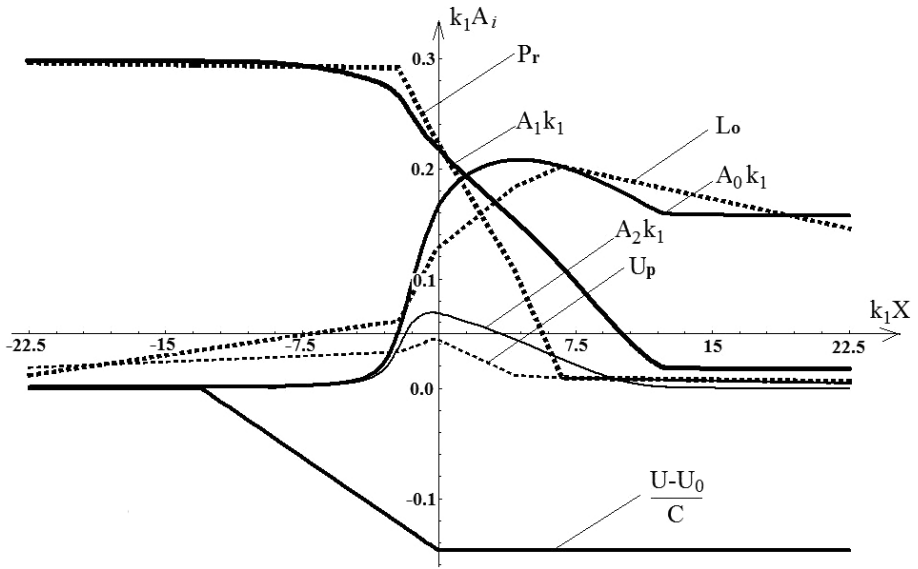

Figure 3. Dashed curves show the zero-dimensional amplitudes of the resonance waves for primary (Pr), lower (Lo) and upper (Up) sidebands obtained experimentally by Chavla and Kirby (2002). The solid lines (A_1, A_0, A_2 respectively) are wave amplitudes calculated in modeling. $(U - U_0)/C$ is the zero-dimensional variable current, where C is the initial phase speed of the carrier wave, $U_0 = -0.32\,\mathrm{m\,s^{-1}}$; $k_1 = 4.71\,\mathrm{m^{-1}}$, $C = 1.44\,\mathrm{m\,s^{-1}}$, $T = 1.2\,\mathrm{s}$.

NPGD
1, 1803–1832, 2014

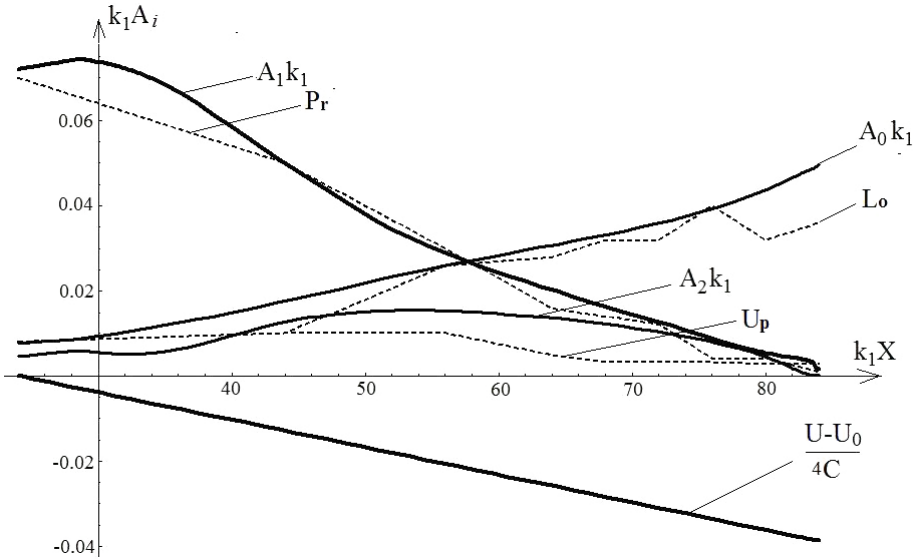

Figure 4. Dashed curves show zero-dimensional amplitudes of the resonance waves for primary (Pr), lower (Lo) and upper (Up) sidebands obtained from experiments conducted by Ma et al. (2010). The solid lines (A_1, A_0, A_2 respectively) are wave amplitudes calculated in modeling. $(U - U_0)/(4C)$ shows the zero-dimensional variable current, where C is the initial phase speed of the primary wave, $U_0 = -0.25\,\mathrm{m\,s^{-1}}; k_1 = 4.1\mathrm{m^{-1}}, C = 1.56\,\mathrm{m\,s^{-1}}, T = 1\,\mathrm{s}$.

NPGD
1, 1803–1832, 2014